Nephrol Dial Transplant (2018) 1–9
doi: 10.1093/ndt/gfy020

ndt
Nephrology Dialysis Transplantation

ORIGINAL ARTICLE

Increased urinary osmolyte excretion indicates chronic kidney disease severity and progression rate

Ryan B. Gil[1], Alberto Ortiz[2], Maria D. Sanchez-Niño[2], Katerina Markoska[3], Eva Schepers[4], Raymond Vanholder[4], Griet Glorieux[4], Philippe Schmitt-Kopplin[1,5,6] and Silke S. Heinzmann[1]

[1]Helmholtz Center Munich, German Research Center for Environment Health, Research Unit Analytical BioGeoChemistry, Neuherberg, Germany, [2] IIS-Fundacion Jimenez Diaz UAM, Madrid, Spain, [3] University of Skopje, Faculty of Medicine, Skopje, Macedonia, [4]Department of Internal Medicine, Nephrology Division, Ghent University Hospital, Ghent, Belgium, [5]German Center for Diabetes Research (DZD), Neuherberg, Germany and [6]Technical University Munich, Chair of Analytical Food Chemistry, Freising-Weihenstephan, Germany

Correspondence and offprint requests to: Silke S. Heinzmann; E-mail: silke.heinzmann@helmholtz-muenchen.de and Philippe Schmitt-Kopplin; E-mail: schmitt-kopplin@helmholtz-muenchen.de

ABSTRACT

Background. Chronic kidney disease (CKD) is a recognized global health problem. While some CKD patients remain stable after initial diagnosis, others can rapidly progress towards end-stage renal disease (ESRD). This makes biomarkers capable of detecting progressive forms of CKD extremely valuable, especially in non-invasive biofluids such as urine. Screening for metabolite markers using non-targeted metabolomic techniques like nuclear magnetic resonance spectroscopy is increasingly applied to CKD research.

Methods. A cohort of CKD patients ($n = 227$) with estimated glomerular filtration rates (eGFRs) ranging from 9.4–130 mL/min/1.73 m^2 was evaluated and urine metabolite profiles were characterized in relation to declining eGFR. Nested in this cohort, a retrospective subset ($n = 57$) was investigated for prognostic metabolite markers of CKD progression, independent of baseline eGFR. A transcriptomic analysis of murine models of renal failure was performed to validate selected metabolomic findings.

Results. General linear modeling revealed 11 urinary metabolites with significant associations to reduced eGFR. Linear modelling specifically showed that increased urine concentrations of betaine ($P < 0.05$) and *myo*-inositol ($P < 0.05$) are significant prognostic markers of CKD progression.

Conclusions. Renal organic osmolytes, betaine and *myo*-inositol play a critical role in protecting renal cells from hyperosmotic stress. Kidney tissue transcriptomics of murine preclinical experimentation identified decreased expression of Slc6a12 and Slc5a11 mRNA in renal tissue consistent with defective tubular transport of these osmolytes. Imbalances in renal osmolyte regulation lead to increased renal cell damage and thus more progressive forms of CKD. Increases in renal osmolytes in urine could provide clinical diagnostic and prognostic information on CKD outcomes.

Keywords: CKD, disease progression, metabolomics, osmolytes, transcriptomics, urine

INTRODUCTION

Chronic kidney disease (CKD) is a term used to include a wide range of diseases that reduce kidney function. The National Kidney Foundation defines CKD as ≥3 months of kidney damage or an estimated glomerular filtration rate (eGFR) <60 mL/min/1.73 m^2 [1]. Disease aetiology in CKD is diverse, leading to variability in morbidity and mortality [2]. Further, not all populations have an equal risk for developing CKD and progressing towards end-stage renal disease (ESRD); therefore, high-risk populations with diabetes and/or hypertension should receive targeted testing for CKD [2]. eGFR can be calculated using the Chronic Kidney Disease Epidemiology Collaboration (CKD-EPI) equation or the Modification of Diet in Renal Disease (MDRD) study equation [1, 2]. However, both measures are relatively insensitive in early stage CKD and their prognostic value is limited.

Novel biomarkers that are more sensitive in early stage CKD are needed for diagnosis and prognosis of CKD progression [3]. Metabolomics can analyse biofluids for specific metabolic signatures reflecting CKD status [4], offering promising non-invasive methods to screen, diagnose and prognose patients for CKD [5–7]. Mass spectrometry (MS) and nuclear magnetic resonance (NMR) are the two main analytical platforms used in metabolomics [8]. Here we use NMR spectroscopy as a quantitative state-of-the-art analytical platform that is widely used in metabolome studies [9]. NMR can detect a wide range of metabolites from various chemical classes, delivering robust transferable data under optimized conditions [10].

The purpose of this study was to use NMR-based metabolomic strategies to elucidate novel urinary markers supportive of current methods for diagnosing CKD. Urine samples from a cohort of 227 patients in various stages of CKD were utilized. An additional aim was to identify prognostic markers that indicate patients at risk of CKD progression towards ESRD. A nested retrospective subgroup ($n = 57$) from the cohort was analysed using follow-up eGFR measurements and a calculated rate of CKD progression.

Results of these analyses point to increased urine concentrations of renal osmolytes as markers of reduced eGFR. These compounds were also significantly elevated in the urine of CKD patients with progressive forms of CKD. These metabolite data were supported with messenger RNA (mRNA) data generated from independent murine kidney fibrosis and injury experimentation.

MATERIALS AND METHODS

Study cohort and sampling

The cohort consisted of patients from the Nephrology Outpatient Clinic at Ghent University Hospital, Ghent, Belgium. Samples were collected in the period 17 January 2011 to 7 July 2015. eGFR was determined using the CKD-EPI equation. Important metadata used in the analysis can be found in Table 1. Sample collection was performed in accordance with local ethics requirements and in accordance with the current revision of the Helsinki Declaration.

A total of 57 patients had sufficient follow-up data to monitor their respective rate of CKD progression (i.e. ≥3 eGFR measurements, minimum of 2-years duration). To reduce confounding factors, only samples from patients with systemic diseases or glomerular diseases were used, and patients with renal transplantation or receiving renal replacement therapy were not considered (Supplementary Table S1). The percent annual eGFR slope change from baseline was calculated using the following equation, an approach that has also been previously applied [11]:

$$\%\ \text{annual eGFR slope} = \frac{\text{linear coefficient}}{\text{baseline eGFR}} \times 100\%$$

Table 1. Urine sample cohort ($n = 227$)

Male, *n* (%)	137 (60.4)
Age (years)	62.3 ± 16.8 (17–88)
Disease groups (*n*, as defined by ERA-EDTA Primary Renal Disease Registry)	
Tubulointerstitial diseases	35
Systemic diseases affecting the kidney[a]	96
Familial/hereditary nephropathies	23
Miscellaneous renal disorders	41
Glomerular diseases	32
Body mass index (kg/m^2)	28.0 ± 5.5 (16.3–47.9)
CKD stage (CKD-EPI, mL/min/1.73 m^2), *n*	
Stage 1 (eGFR >90)	25
Stage 2 (eGFR 89–60)	45
Stage 3 (eGFR 59–30)	115
Stage 4 (eGFR 29–15)	34
Stage 5 (eGFR <15)	8
eGFR (mL/min/1.73 m^2)	51 ± 25.7 (9.4–130)

This table provides an overview of cohort metadata used for biomarker discovery. Age, gender, BMI and CKD disease groups were determined to be the most important metadata in linear modelling of metabolites. For age, BMI and eGFR, the mean and standard deviation are shown with the range.

[a]Systemic diseases includes diabetes type 2 and hypertension.

Sample preparation for NMR and instrumental protocol

Upon collection, urine samples were immediately centrifuged (20800 *g* for 10 min), aliquoted per 1 mL and stored at −80°C. Following defrosting, a buffering approach designed for NMR analysis in urine was applied [12]. This included a deuterium oxide phosphate buffer (1.5 M PO_4, pH 7.4; Armar Chemicals, Leipzig, Germany) with potassium fluoride (KF, 300 mM) and (trimethylsilyl)propionic acid (TSP, 0.1%). Phosphate salts, KF and TSP were purchased from Sigma Aldrich Chemie (Steinheim, Germany).

Urine samples were analysed on a Bruker 800-MHz spectrometer operating at 800.35 MHz with a quadrupole inverse cryogenic probe. A standard one-dimensional pulse sequence [recycle delay (RD) 90°, t1 90°, tm 90°, acquire FID] was acquired, with water suppression irradiation during RD of 2 s, mixing time (tm) set on 200 ms and a 90° pulse set to 10.13 µs, collecting 512 scans into 64 000 data points with a spectral width of 12 ppm. All spectra were manually phased, baseline corrected and calibrated to TSP (δ 0.00) with TopSpin 3.2 (Bruker BioSpin, Rheinstetten, Germany). Data were imported to MATLAB (MathWorks, Natick, MA, USA) and further processed, i.e., water and urea region removed (δ 4.7–5.6). Daily quality control samples (i.e. pooled urine sample) were measured throughout the cohort measurement to monitor instrument performance, data processing (i.e. spectra pre-processing, normalization and alignment) and metabolite stability.

The structural identity of metabolite compounds was determined by two-dimensional (2D) NMR methods; total correlation spectroscopy (TOCSY) and heteronuclear single quantum coherence (HSQC) spectroscopy. For 2D TOCSY spectra, phase-sensitive and sensitivity-improved 2D TOCSY with WATERGATE (3-9-19) and DIPSI-2 were acquired. For each spectrum 19228 × 1024 data points were collected using 32 scans per increment, 16 dummy scans and 1 s acquisition time. The spectral widths were set to 12 ppm for both the F1 and F2 dimensions. For 2D HSQC spectra, phase-sensitive ge-2D HSQC using PEP and adiabatic pulses for inversion and refocusing with gradients was used. Data points of 4788 × 1280 per spectra were collected with 256 scans per increment, 16 dummy scans and an acquisition time of 0.25 s. Spectral widths were set to 12 ppm for the F2 and 230 ppm for F1.

NMR-based statistical tools

Data processing and statistics were performed in MATLAB 2015b, RStudio and the MetaboAnalyst platform (http://www.metaboanalyst.ca) [13]. Probabilistic quotient normalization [14] was used for normalization of spectral data to account for biological variation in urine dilution. This method is an improved normalization technique compared with single-metabolite normalization [15], which is superior in the context of CKD, as it avoids normalization to metabolites affected by

the disease. Spectral data were aligned using the recursive segment-wise peak alignment (RSPA) algorithm [16]. An orthogonal partial least squares (OPLS) regression analysis [17] using eGFR as the y variable was performed for spectral feature selection. Spectral regions most affected by CKD display high covariance and r^2 values. Selected spectral features were structurally identified using 2D NMR and matched with the human metabolite database (HMDB) [18]. Identified metabolites were quantified with the R-package BATMAN [19], measuring the area under the curve. Data were then log transformed and mean centered. General linear modelling was applied to each identified metabolite with baseline eGFR or percent annual eGFR slope as y variables, adjusted for age, gender, body mass index (BMI) and disease group.

Kidney transcriptomics

Total RNA was isolated using the PureLink RNA Mini Kit (Invitrogen, Paisley, UK). Affymetrix transcriptomics arrays of kidney tissue ($n = 3$ control and $n = 3$ kidney injury, obtained 24 h after induction of kidney injury by a folic acid injection or injection of vehicle) were performed at Unidad Genómica Moncloa, Fundación Parque Científico de Madrid, Madrid, Spain, following the manufacturer's protocol [20]. Image files were initially obtained through Affymetrix GeneChip Command Console software. Robust multichip analysis was performed using the Affymetrix Expression Console software. Starting from the normalized robust multichip analysis, the significance analysis of microarrays was performed using the limma package (Babelomics, http://www.babelomics.org), with a false discovery rate (FDR) of 5% to identify genes significantly dysregulated.

Experimental kidney injury

These studies were approved by the IIS-FJD animal ethics committee and followed Directive 2010/63/EU on the protection of animals used for scientific purposes. For experimental kidney injury, female 12- to 14-week-old C57/BL6 mice received a single intraperitoneal injection of folic acid (Sigma Aldrich) 250 mg/kg in sodium bicarbonate 0.3 mol/L (acute kidney injury, $n = 3$) or a vehicle alone (controls, $n = 3$) and were sacrificed 24 h later as previously described [20]. Kidneys were cold saline perfused *in situ* before removal. One kidney from each mouse was fixed in buffered formalin, embedded in paraffin and stained with haematoxylin and eosin. The other kidney was snap frozen in liquid nitrogen for ribonucleic acid (RNA) studies. Samples from this experiment were used for kidney transcriptomics. A second set of six mice per group with folic acid nephropathy or vehicle-infused controls were processed in the same manner at 24 and 72 h following the induction of kidney injury and used for real-time quantitative polymerase chain reaction (qPCR) validation.

Unilateral ureteral obstruction (UUO) was performed under isoflurane-induced anaesthesia. The left ureter was ligated with silk at two locations and cut to prevent urinary tract infection (obstructed kidney) [21]. A total of five male 12- to 14-week-old C57/BL6 mice were sacrificed 14 days after surgery. UUO kidneys were compared with the healthy contralateral kidneys.

Real-time qPCR validation

Human metabolomics and murine transcriptomics results were validated by real-time qPCR performed using mRNA obtained from five UUO mice sacrificed on Day 14 and from folic acid nephropathy mice vehicle-infused controls obtained at 24 and 72 h following induction of kidney injury. RNA of 1 µg isolated by Trizol (Invitrogen) was reverse transcribed with a High Capacity cDNA Archive Kit and real-time qPCR was performed on a ABI Prism 7500 PCR system (Applied Biosystems, Foster City, CA, USA) using the ΔΔCt method [22]. Expression levels are displayed as ratios to glyceraldehyde-3-phosphate dehydrogenase. Pre-developed primer and probe assays were also from Applied Biosystems.

Data mining

The Nephroseq [http://www.nephroseq.org/ (11 October 2017, date last accessed)] database was searched for human renal biopsy transcriptomics data comparing patients with diverse aetiologies of CKD with controls. The database was searched for gene expression data for *Slc5a11*, *Slc6a12* and *Slc5A3*. Supplementary Figure S1 shows the experimental workflow.

RESULTS

Urine metabolite markers related to eGFR

An OPLS regression analysis of the entire cohort data set measured by ^{1}H NMR revealed spectral features with significant linear relationship to eGFR (Figure 1). Spectral features with the largest absolute covariance and r^2 values (Figure 1C) were targeted for identification and quantification (Figure 1A). A list of the identified metabolites can be found in Supplementary Table S2. General linear modelling of all quantified metabolites showed 11 urinary metabolites having significant linear associations with eGFR, adjusted for age, gender, BMI and disease group (Table 2). A positive association with decreased eGFR reflects a decrease in the relative concentration of each respective metabolite as eGFR declines.

Metabolites from various metabolic pathways were altered with reduced eGFR. Citric acid from the tricarboxylic acid cycle, amino acids (e.g. threonine), lipid metabolism (e.g. ethanolamine), gut microbiome–derived uraemic toxins (e.g. indoxyl sulphate and *p*-cresol sulphate), uracil and glycolic acid were significantly lower with reduced eGFR. Many of these metabolites have also been reported as significant markers of CKD from previous studies [23–25], further strengthening them as reliable biomarkers. Additionally, two metabolites, *myo*-inositol and betaine, had negative coefficients, indicating a respective urinary increase with reduced eGFR.

Metabolite markers related to CKD progression

A nested retrospective subgroup ($n = 57$) of the cohort was analysed for urine metabolites predictive of CKD progression. These CKD patients were well distributed throughout the range of progression ($r^2 = 0.96$), which was from 5% per year (i.e. improvement in eGFR) to −14.1% per year (i.e. strong deterioration) (Supplementary Figure 2). The percent annual eGFR slope was independent of baseline eGFR ($P = 0.44$) (Supplementary Figure

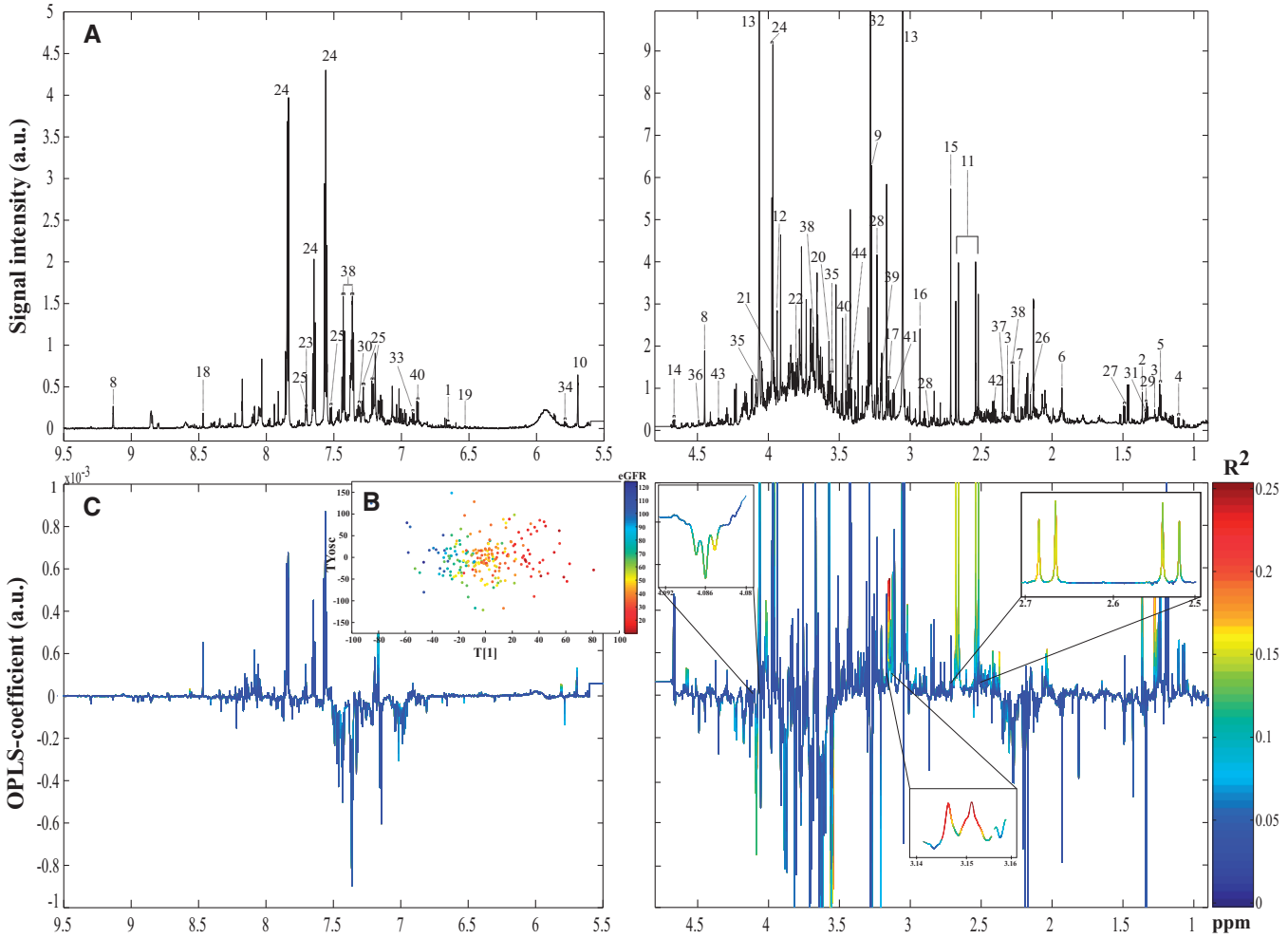

FIGURE 1: OPLS regression analysis for feature selection in NMR spectra. **(A)** Sample spectrum with identified metabolites labelled: (1) 2-furoylglycine, (2) 2-hydroxyisobutyric acid, (3) 3-hydroxyisovaleric acid, (4) 4-deoxyerythronic acid, (5) 4-deoxytheonic acid, (6) acetic acid, (7) acetone, (8) trigonelline, (9) betaine, (10) *cis*-aconitic acid, (11) citric acid, (12) creatine, (13) creatinine, (14) D-glucose, (15) dimethylamine, (16) dimethylglycine, (17) ethanolamine, (18) formic acid, (19) fumaric acid, (20) glycine, (21) glycolic acid, (22) guanidoacetic acid, (23) pseudouridine, (24) hippuric acid, (25) indoxyl sulfate, (26) L-acetylcarnitine, (27) L-alanine, (28) trimethylamine, (29) L-lactic acid, (30) L-phenylalanine, (31) L-threonine, (32) trimethylamine-*N*-oxide, (33) L-tyrosine, (34) uracil, (35) *myo*-inositol, (36) *N*-methylnicotinamide, (37) *p*-cresol sulfate, (38) phenylacetylglutamine, (39) phosphorylcholine, (40) *p*-hydroxyphenylacetic acid, (41) proline betaine, (42) succinic acid, (43) tartaric acid and (44) taurine. **(B)** Loadings plot of OPLS regression analysis with eGFR in the *y* variable. This plot represents a 'statistical' pseudo-spectrum that displays the OPLS model covariance on the *y*-axis and chemical shift on the *x*-axis. The colour bar represents the r^2 value for that spectral region to eGFR. Plots in (A) and (B) are aligned on the *x*-axis, which shows which spectral regions may best describe CKD-related changes and warrant structural identification. **(C)** Scores plot of the OPLS model showing data separation based on sample eGFR (colour bar).

S3). Linear modelling was again applied using the percent annual eGFR slope change as the *y* variable. A total of eight metabolites showed significant associations (Table 3). Citric acid, glycolic acid and ethanolamine were again seen to be positively associated with a declining percent annual eGFR slope. Creatinine and dimethylamine were also positively associated. The highest β coefficients in the modelling were seen for betaine and *myo*-inositol, which had negative correlations (Figure 2). These osmolytes again showed opposite trends from all other significant metabolites.

Due to the longitudinal nature of the sample group, the previously mentioned metabolites may act as prognostic urinary biomarkers of CKD outcome. We focused on to examining the renal osmolytes betaine and *myo*-inositol, as their respective trends were contrary to the other metabolites and their physiological relevance in kidney health is unique. Using receiver operating characteristics (ROC) analysis, the values of betaine and *myo*-inositol were examined in the first and last quartiles of the CKD progression subgroup. Here, the first quartile (i.e. 'stable') showed no CKD progression, with an eGFR change of +5% to −1% per year. The last quartile (i.e. 'rapid' progression) showed an eGFR change of −8% to −15% per year. The area under the curve (AUC) of the ROC analysis for betaine was 0.814 and for *myo*-inositol was 0.781. Combined, both betaine and *myo*-inositol showed an AUC of 0.84 (Supplementary Figure S4).

Decreased kidney expression of betaine and *myo*-inositol transporters in murine models

To determine if osmolyte transporters were a factor for increased urine osmolyte concentrations, kidney transcriptomics of a murine CKD model were analysed for gene expression

changes. The kidney gene expression of *Slc5a3*, *Slc5a11* and *Slc6a12* (see Figure 3) was assessed by real-time qPCR in experimental kidney fibrosis induced by UUO, a classic murine model of renal fibrosis and inflammation that recapitulates all the key events in CKD leading to fibrosis [26]. Significant downregulation of the genes encoding the *myo*-inositol transporter (*Slc5a11*) and the betaine transporter (*Slc6a12*) were observed (Figure 4A).

The candidate genes (*Slc5a3*, *Slc5a11*, *Slc6a12*) tested in experimental CKD were also observed in a transcriptomics analysis of kidney injury using a murine model injected with folic acid. Supplementary Table S3 shows all differentially expressed genes in the transcriptomics array with a fold change increasing or decreasing in expression >25% and FDR <5%, as previously reported [27]. Our hypothesis-driven analysis of the transcriptomics database identified decreased expression of *Slc6a12*, *Slc5a3* and *Slc5a11* (Figure 4B). Downregulation of these genes did not appear to result from the downregulation of the transcription factor tonicity-responsive enhancer-binding protein (TonEBP/NFAT5), a master regulator of osmolyte transporters, since TonEBP/NFAT5 expression was preserved (fold change 0.96, FDR = ns). Additionally, *Myox*, the gene encoding *myo*-inositol oxygenase, was also downregulated in kidney injury (Supplementary Figure S5). Real-time qPCR confirmed in an independent validation experiment of the decreased expression of *Slc5a3*, *Slc5a11* and *Slc6a12* mRNA at 24 h of kidney injury induction and persisting after 72 h (Figure 4C). These data suggest that these gene expression changes are shared by both CKD and acute kidney injuries.

Table 2. Significant diagnostic metabolites of eGFR

Metabolite	β	SE	P-value
Citric acid	0.023	0.003	3.42E-10
Uracil	0.02	0.004	3.25E-07
Formic acid	0.01	0.002	4.76E-05
L-threonine	0.016	0.005	3.15E-03
Ethanolamine	0.004	0.001	3.61E-03
myo-Inositol	−0.014	0.005	6.12E-03
Glycolic acid	0.014	0.005	1.14E-02
Indoxyl sulphate	0.009	0.004	1.53E-02
Hippuric acid	0.011	0.004	1.57E-02
p-Cresol sulphate	0.014	0.006	3.03E-02
Betaine	−0.013	0.006	4.79E-02

This table shows general linear modelling results for diagnostic markers of baseline eGFR. These metabolites show significant linear associations with eGFR. The β coefficient, standard error (SE) and P-value for each metabolite are reported and are adjusted for age, gender, BMI and CKD disease group. Metabolites with a negative correlation (i.e. negative β) indicate metabolites that have increased urinary concentration as eGFR declines.

Table 3. Significant prognostic metabolites of CKD progression

Metabolite	β	SE	P-value
Creatinine	0.059	0.011	3.57E-06
Citric acid	0.079	0.027	0.005
Ethanolamine	0.039	0.014	0.010
Betaine	−0.153	0.057	0.010
Trimethylamine *N*-oxide	−0.053	0.022	0.022
Dimethylamine	0.025	0.011	0.025
Glycolic acid	0.09	0.041	0.031
myo-Inositol	−0.091	0.042	0.035

This table shows general linear modelling results for prognostic markers of CKD progression. These metabolites show significant linear associations with percent annual eGFR slope of the selected progression subset. The β coefficient, standard error (SE) and P-value of each metabolite are reported and are adjusted for age, gender, BMI and CKD disease group A negative association (i.e. negative β) indicates an increase in the metabolite concentration as the percent annual eGFR slope decreases (i.e. CKD progression rate increases).

DISCUSSION

In the present study we investigated the urine metabolome signatures of patients with CKD and CKD progression. Most significant metabolites decrease in urinary concentration with reduced eGFR and in patients with progressing CKD. However, in these same patients we also observed significant linear increases of *myo*-inositol and betaine. Both metabolites had the highest absolute β coefficients in our modelling of percent annual eGFR slope and showed prognostic value in predicting patients who rapidly progress from those who remained stable. Kidney transcriptomics identified defective gene expressions of *myo*-inositol and betaine transporters in

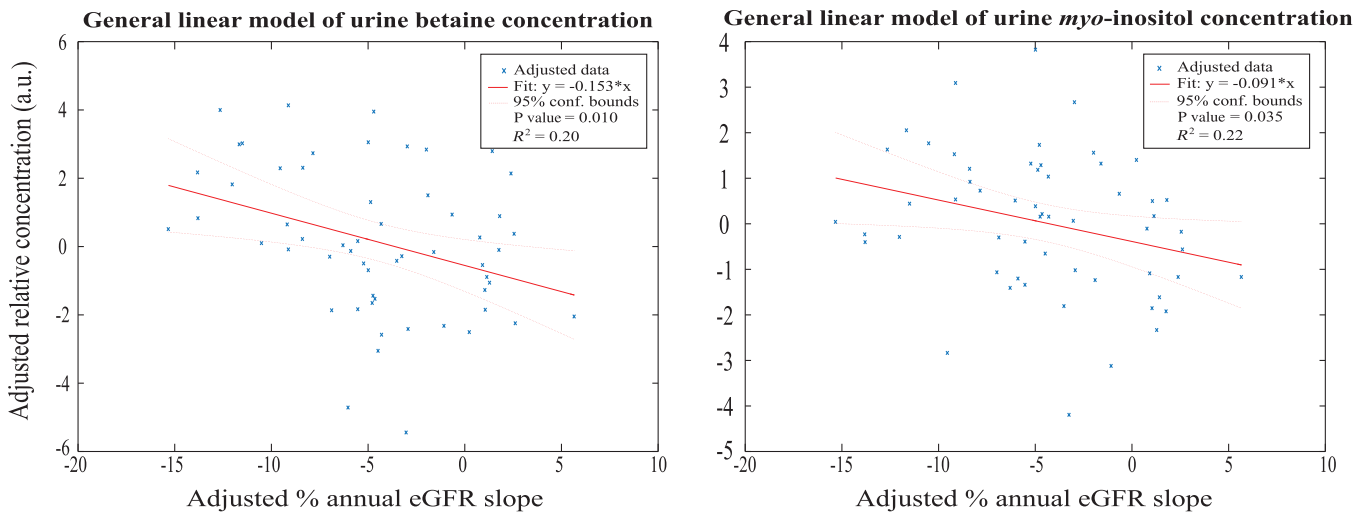

FIGURE 2: Plots of adjusted generalized linear model for renal osmolytes. A negative percent annual eGFR slope indicates patients that are progressing in CKD. The linear model equation, 95% confidence intervals and P-values are defined in the legend.

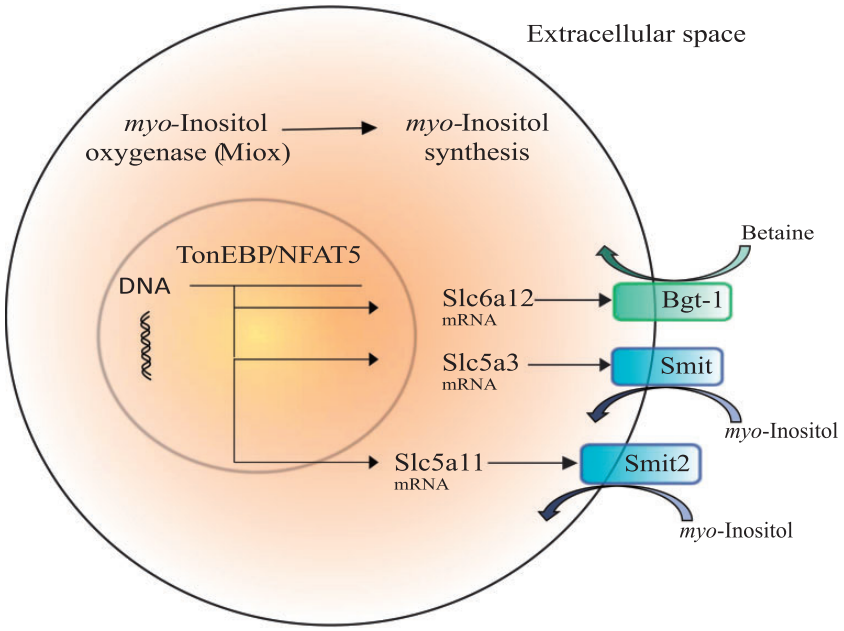

FIGURE 3: Function of gene products in tubular cells. *Slc6a12* encodes the betaine transporter bgt-1. *Slc5a3* encodes the sodium *myo*-inositol transporter Smit. *Slc5a11* encodes the sodium *myo*-inositol transporter Smit2. *Myox* encodes *myo*-inositol oxygenase, which is involved in *myo*-inositol synthesis. Transcription factor TonEBP/Nfat5 regulates gene expression of all osmolyte transporter genes; (*Slc6a11*, *Slc5a3*, and *Slc5a11*).

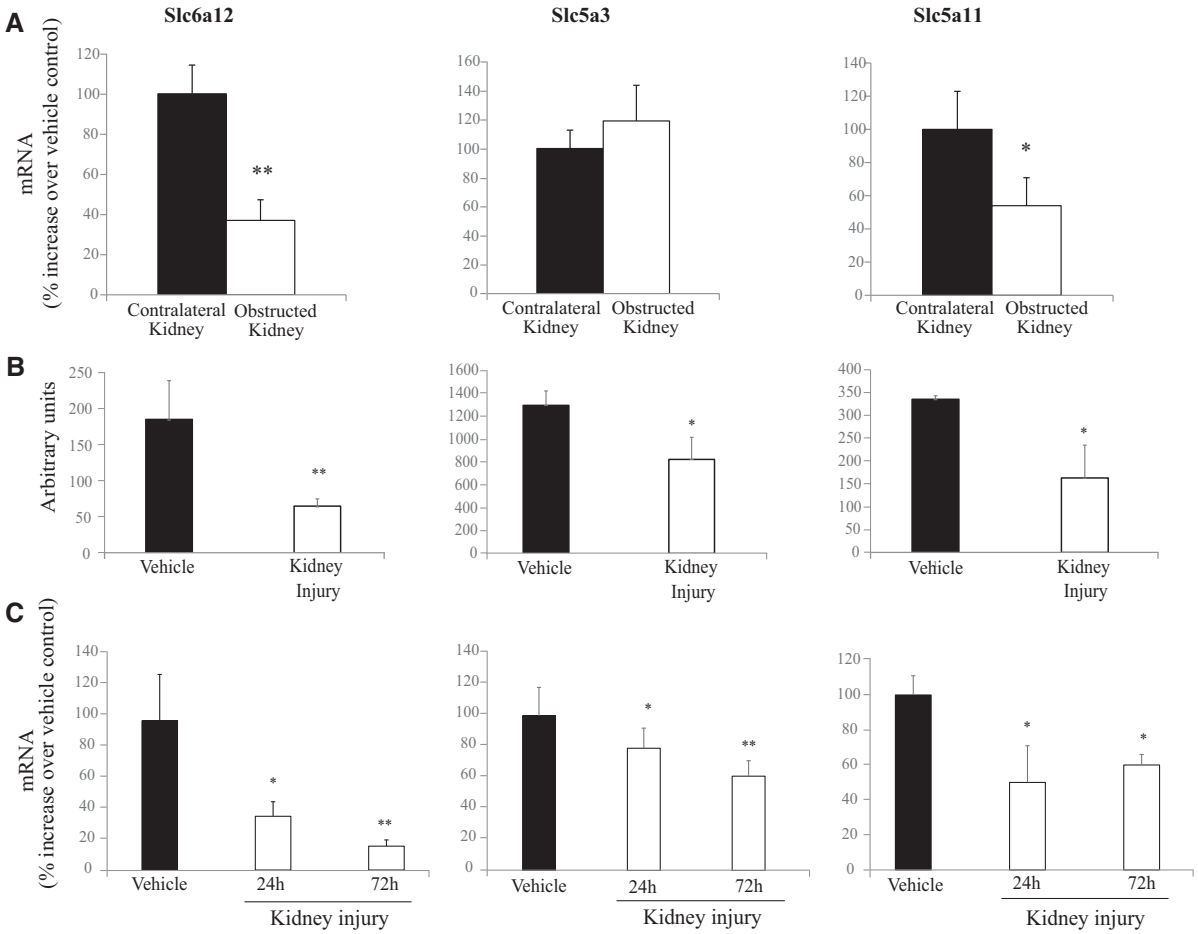

FIGURE 4: Gene expression data. (**A**) Changes in experimental kidney fibrosis assessed by real-time qPCR. Kidney mRNA was measured 14 days after induction of UUO leading to kidney fibrosis. Obstructed kidneys were compared with contralateral unobstructed kidneys. (**B**) Changes in experimental kidney injury transcriptomics. Kidney mRNA was measured 24 h after induction of kidney injury by a single injection of folic acid and in vehicle-injected controls. (**C**) Changes in experimental kidney injury assessed by real-time qPCR. Kidney mRNA was measured 24 h and 72 h after induction of kidney injury by a single injection of folic acid and in vehicle-injected controls. *P $\leq$ 0.05, **P $\leq$ 0.01.

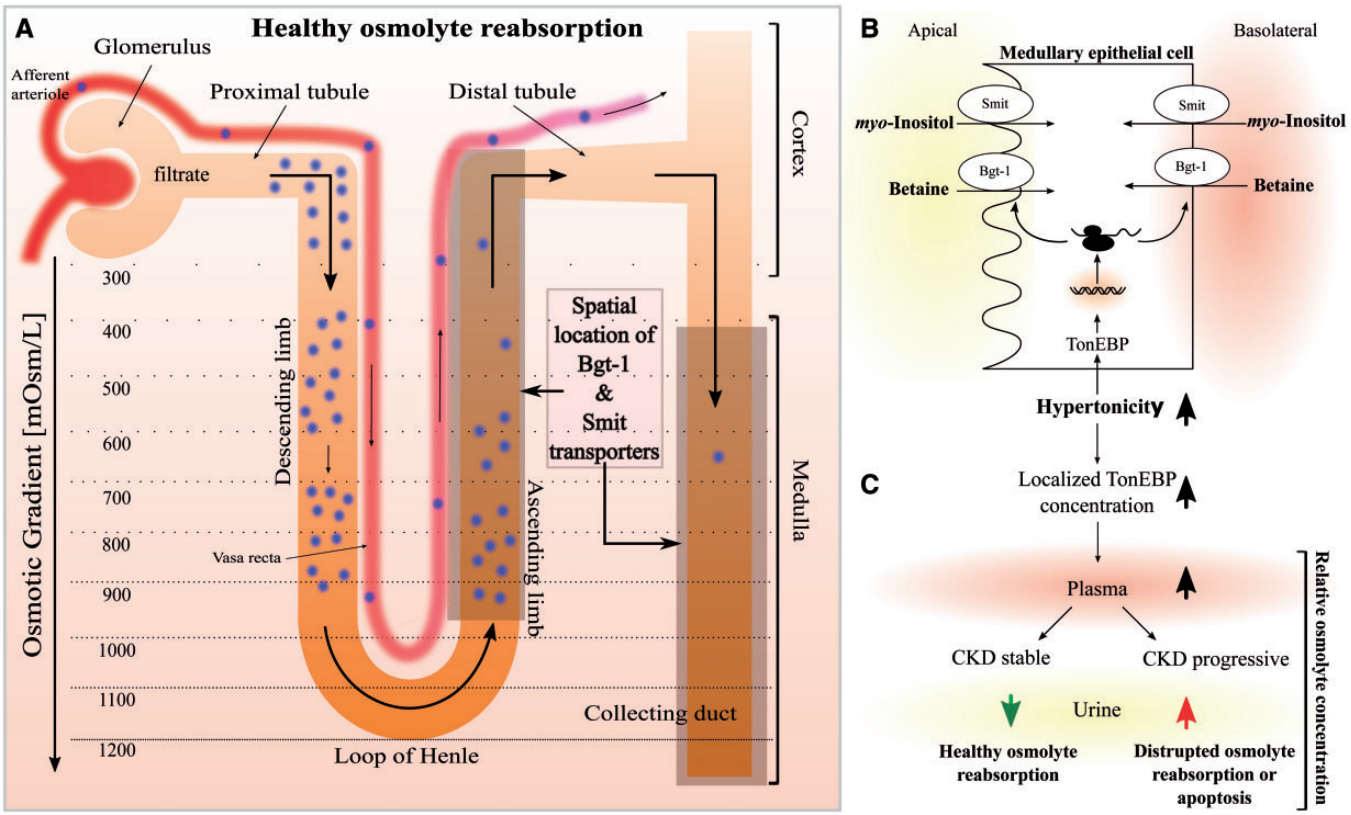

FIGURE 5: Hypertonicity response mechanism in CKD. A proposed model of the osmolyte mechanism in CKD. **(A)** Model of osmolyte reabsorption in a healthy nephron. **(B)** Tubular cell response mechanism to increased hypertonicity in medullary tissue. **(C)** Blood and urine osmolyte concentrations in response to hypertonicity. Patients with progressive forms of CKD have increased osmolyte concentrations in urine.

murine kidney disease models, providing convincing evidence that elevated osmolyte concentrations seen in the urine are partially a result of perturbed renal osmolyte transport. Figure 5 provides a proposed model of osmolyte dysregulation during CKD. This may be the first demonstration that links urinary osmolyte concentrations with clinical CKD outcomes using a metabolomic analysis supported with transcriptomics.

The osmolality of mammalian blood is normally kept constant at ∼290 mosmol/kg [28] and maintained by regulatory mechanisms such as the renin–angiotensin–aldosterone and antidiuretic hormone systems. However, normal kidney function requires an interstitial osmotic gradient in renal medulla four times that of plasma osmolality. The hyperosmotic conditions created by NaCl and urea are required for urine concentration. However, these conditions can be damaging to cells and proteins [28, 29] and cause water to diffuse out of cells, resulting in cellular shrinkage [30]. Osmolytes have evolved in renal tissues as protective compounds against osmotic stress [31], and studies have explored mechanisms for how osmolytes provide protein stability [32, 33]. Five protective osmolytes are used in renal cells: sorbitol, betaine, *myo*-inositol, taurine and glycerophosphocholine (GPC), with a large proportion being betaine and *myo*-inositol [28, 29]. The concentrations of these osmolytes are regulated through the TonEBP/NFAT5 transcription factor [28, 34], which regulates the transcription of all transporter proteins responsible for osmolyte uptake in renal cells. This transcription factor is critical to kidney health and has been proven essential in knockout models [30, 35].

Mechanisms for betaine uptake in medullary cells are well studied [28, 36]. As osmolality increases, so too do medullary betaine levels [28, 37]. Uptake comes primarily from extracellular sources and not from increased local cellular synthesis [28]. Betaine is freely filtered by glomeruli and actively reabsorbed by renal tubules at levels >95% of the filtered load [38, 39] (Figure 5A). Therefore, non-perturbed reabsorption mechanisms for betaine should not allow for an increase in urinary levels as seen in our study. The primary transporter of betaine in medullary cells is betaine/GABA transporter 1 (Bgt-1) [28, 40], which is encoded by the *Slc6a12* gene and regulated by TonEBP/NFAT5 [30]. Hypertonicity leads to increased TonEBP/NFAT5 expression and localization of Bgt-1 to apical and basolateral plasma membranes in tubular cells (Figure 5B). It is estimated that betaine could account for ∼25% of the total osmolyte content [40, 41], and a recent study found that betaine ranked high in protein-stabilizing properties [32]. Its high abundance and stabilizing properties provide evidence that betaine is one of the more important organic osmolytes in medullary tissues. A recent study of acute renal ischaemia found kidney tissue had reduced levels of betaine and *myo*-inositol when compared with controls [42, 43]. Therefore, increased betaine in the urine most likely reflects CKD-related renal stress

(Figure 5C). Our data show an increase of betaine in human urine during CKD, most likely due to Bgt-1 transporter downregulation, given the lower gene expression in experimental kidney fibrosis and injury. However, the release of osmolytes into the urine following renal cell damage may also contribute.

Myo-inositol also increases in healthy medullary cells when interstitial osmolality increases, and reduced *Myox* gene expression in experimental kidney injury argues against increased local *myo*-inositol production being a major driver of higher urinary levels in CKD. Sodium *myo*-inositol transporters (Smit and Smit2) encoded by the *Slc5a3* and *Slc5a11* genes are primarily responsible for renal *myo*-inositol uptake [28] and are also regulated by TonEBP/NFAT5 [30]. Downregulation of *Slc5a11* was observed in experimental kidney fibrosis, and *Slc5a3* and *Slc5a11* were also downregulated during kidney injury, suggestive of a general decrease in *myo*-inositol uptake capacity by stressed tubular cells. Furthermore, a recent study found *myo*-inositol significantly elevated in the urine of mice with renal vasculitis [44].

We hypothesize that increased urinary levels of renal osmolytes reflect damage to kidney tissue from hyperosmolar stress, especially in diseases such as diabetic and hypertensive nephropathy, where osmotic and hypertensive stresses cause microvasculature damage [35, 45]. In support, gene expression data of osmolyte transporters point to a dysregulated transporter system as a major factor of osmolytes lost into the urine. Data mining of human kidney biopsy gene expression using the Nephroseq database (www.Nephroseq.org) showed a study exploring gene expression in human CKD with diverse aetiologies [46]. These data identified the downregulated kidney expression of *Slc5a11* (foldchange −3.15 discovery, −1.91 validation) and *Slc6a12* (foldchange −1.63 discovery, −6.98 validation) mRNA in human CKD kidneys compared with control kidneys. However, no difference in *Slc5a3* mRNA expression was observed, as was similarly seen in our experimental kidney fibrosis data.

The present data are consistent with the increased recognition of osmotic stress as a driving force behind CKD progression. For example, repeated dehydration and osmotic stress are thought to be a key driver of kidney injury in Meso-American nephropathy patients [47]. Moreover, tolvaptan, an antagonist of antidiuretic hormone receptors that promotes polyuria and decreases medullary hyperosmolarity, has been recently approved to treat polycystic kidney disease. Experimental evidence suggests that tolvaptan or high water intake may be protective in other nephropathies [48]. Finally, data consistent with impaired kidney responses to osmotic stress in CKD are in line with clinical observations that CKD patients are more sensitive to the toxic effects of high-osmolality iodinated contrast media [49].

There are certain limitations in our study. The number of samples in the CKD progression analysis is somewhat low, and a larger, multicentre, validation study is warranted. However, betaine and *myo*-inositol showed the same significant direction of alteration in the larger-scale analysis of the total cohort eGFR. Furthermore, gene expression data from independent experimental murine models provides interdiscipline validation of the pathophysiological feasibility of osmolyte abnormalities acting as CKD progression biomarkers. Therefore, the increased urinary output of betaine and *myo*-inositol reflects abnormal tubular transport of osmolytes and an impaired renal medullary response to osmotic stress in CKD progression.

SUPPLEMENTARY DATA

Supplementary data are available at ndt online.

FUNDING

The research leading to these results has received funding from the European Union's Seventh Framework Programme FP7/2007-2013 under grant agreement FP7-PEOPLE-2013-ITN-608332. A.O. and M.D.S.N. were supported by Spanish government FEDER funds RETIC REDINREN RD016/0019. FIS PI16/02057, PI15/00298, CP14/00133, Sociedad Española de Nefrología, Programa Intensificacion Actividad Investigadora (ISCIII/Agencia Lain-Entralgo/CM), Miguel Servet MS14/00133.

CONFLICT OF INTEREST STATEMENT

A.O. reports grants from the Spanish government during the conduct of the study.

REFERENCES

1. Inker LA, Astor BC, Fox CH *et al.* KDOQI US commentary on the 2012 KDIGO clinical practice guideline for the evaluation and management of CKD. *Am J Kidney Dis* 2014; 63: 713–735
2. Vassalotti JA, Centor R, Turner BJ *et al.* Practical approach to detection and management of chronic kidney disease for the primary care clinician. *Am J Med* 2016; 129: 153–162.e7
3. Slocum JL, Heung M, Pennathur S. Marking renal injury: can we move beyond serum creatinine? *Transl Res* 2012; 159: 277–289
4. Wettersten HI, Weiss RH. Applications of metabolomics for kidney disease research. *Organogenesis* 2013; 9: 11–18
5. Weiss RH, Kim K. Metabolomics in the study of kidney diseases. *Nat Rev Nephrol* 2011; 8: 22–33
6. Hocher B, Adamski J. Metabolomics for clinical use and research in chronic kidney disease. *Nat Rev Nephrol* 2017; 13: 269–284
7. Zhao Y-Y, Xu Q. Metabolomics in chronic kidney disease. *Clin Chim Acta* 2013; 422: 59–69
8. Zhao YY, Cheng XL, Vaziri ND *et al.* UPLC-based metabonomic applications for discovering biomarkers of diseases in clinical chemistry. *Clin Biochem* 2014; 47: 16–26
9. Heinzmann SS, Merrifield C. A, Rezzi S *et al.* Stability and robustness of human metabolic phenotypes in response to sequential food challenges. *J Proteome Res* 2012; 11: 643–655
10. Dona AC, Jimenez B, Schäfer H *et al.* Precision high-throughput proton NMR spectroscopy of human urine, serum, and plasma for large-scale metabolic phenotyping. *Anal Chem* 2014; 86: 9887–9894
11. Schanstra JP, Zürbig P, Alkhalaf A *et al.* Diagnosis and prediction of CKD progression by assessment of urinary peptides. *J Am Soc Nephrol* 2015; 26: 1999–2010
12. Gil RB, Lehmann R, Schmitt-Kopplin P *et al.* ^{1}H NMR-based metabolite profiling workflow to reduce inter-sample chemical shift variations in urine samples for improved biomarker discovery. *Anal Bioanal Chem* 2016; 408: 4683–4691
13. Xia J, Wishart DS. Using MetaboAnalyst 3.0 for comprehensive metabolomics data analysis. *Curr Protoc Bioinform* 2016; 55: 14.10.1–14.10.91
14. Dieterle F, Ross A, Schlotterbeck G *et al.* Probabilistic quotient normalization as robust method to account for dilution of complex biological mixtures. Application in ^{1}H NMR metabonomics. *Anal Chem* 2006; 78: 4281–4290

15. Kohl SM, Klein MS, Hochrein J *et al.* State-of-the art data normalization methods improve NMR-based metabolomic analysis. *Metabolomics* 2012; 8: 146–160
16. Veselkov KA, Lindon JC, Ebbels TMD *et al.* Recursive segment-wise peak alignment of biological ^{1}H NMR spectra for improved metabolic biomarker recovery. *Anal Chem* 2009; 81: 56–66
17. Cloarec O, Dumas M, Craig A *et al.* Statistical total correlation spectroscopy: an exploratory approach for latent biomarker identification from metabolic ^{1}H NMR data sets statistical total correlation spectroscopy: an exploratory approach for latent biomarker identification from metabolic. *Anal Chem* 2005; 77: 1282–1289
18. Wishart DS, Jewison T, Guo AC *et al.* HMDB 3.0—the human metabolome database in 2013. *Nucleic Acids Res* 2012; 41: D801–D807
19. Hao J, Liebeke M, Astle W *et al.* Bayesian deconvolution and quantification of metabolites in complex 1D NMR spectra using BATMAN. *Nat Protoc* 2014; 9: 1416–1427
20. Izquierdo MC, Sanz AB, Mezzano S *et al.* TWEAK (tumor necrosis factor–like weak inducer of apoptosis) activates CXCL16 expression during renal tubulointerstitial inflammation. *Kidney Int* 2012; 81: 1098–1107
21. Ucero AC, Benito-Martin A, Fuentes-Calvo I *et al.* TNF-related weak inducer of apoptosis (TWEAK) promotes kidney fibrosis and Ras-dependent proliferation of cultured renal fibroblast. *Biochim Biophys Acta* 2013; 1832: 1744–1755
22. Ortiz A, Husi H, Gonzalez-Lafuente L *et al.* Mitogen-activated protein kinase 14 promotes AKI. *J Am Soc Nephrol* 2017; 28: 823–836
23. Chen DQ, Cao G, Chen H *et al.* Gene and protein expressions and metabolomics exhibit activated redox signaling and wnt/β-catenin pathway are associated with metabolite dysfunction in patients with chronic kidney disease. *Redox Biol* 2017; 12: 505–521
24. Posada-Ayala M, Zubiri I, Martin-Lorenzo M *et al.* Identification of a urine metabolomic signature in patients with advanced-stage chronic kidney disease. *Kidney Int* 2014; 85: 103–111
25. Raffler J, Friedrich N, Arnold M *et al.* Genome-wide association study with targeted and non-targeted NMR metabolomics identifies 15 novel loci of urinary human metabolic individuality. *PLoS Genet* 2015; 11: e1005487
26. Ucero AC, Benito-Martin A, Izquierdo MC *et al.* Unilateral ureteral obstruction: beyond obstruction. *Int Urol Nephrol* 2014; 46: 765–776
27. Martin-Lorenzo M, Gonzalez-Calero L, Ramos-Barron A *et al.* Urine metabolomics insight into acute kidney injury point to oxidative stress disruptions in energy generation and H_2S availability. *J Mol Med* 2017; 95: 1399–1409
28. Burg MB, Ferraris JD. Intracellular organic osmolytes: function and regulation. *J Biol Chem* 2008; 283: 7309–7313
29. Yancey PH. Organic osmolytes as compatible, metabolic and counteracting cytoprotectants in high osmolarity and other stresses. *J Exp Biol* 2005; 208: 2819–2830
30. Lopez-Rodriguez C, Antos CL, Shelton JM *et al.* Loss of NFAT5 results in renal atrophy and lack of tonicity-responsive gene expression. *Proc Natl Acad Sci USA* 2004; 101: 2392–2397
31. Yancey PH, Clark ME, Hand SC *et al.* Living with water stress: evolution of osmolyte systems. *Science* 1982; 217: 1214–1222
32. Street TO, Bolen DW, Rose GD. A molecular mechanism for osmolyte-induced protein stability. *Proc Natl Acad Sci USA* 2006; 103: 13997–14002
33. Katayama H, McGill M, Kearns A *et al.* Strategies for folding of affinity tagged proteins using GroEL and osmolytes. *J Struct Funct Genomics* 2009; 10: 57–66
34. Day CR, Gordon SS, Vaughn CL *et al.* A single amino acid substitution in the renal betaine/GABA transporter prevents trafficking to the plasma membrane. *Physiol J* 2013; 2013: 1
35. Brocker C, Thompson DC, Vasiliou V. The role of hyperosmotic stress in inflammation and disease. *Biomol Concepts* 2012; 3: 345–364
36. Burg MB. Coordinate regulation of organic osmolytes in renal cells. *Kidney Int* 1996; 49: 1684–1685
37. Nakanishi T, Turner RJ, Burg MB. Osmoregulation of betaine transport in mammalian renal medullary cells. *Am J Physiol* 1990; 258: F1061–F1067
38. Lever M, Sizeland PCB, Bason LM *et al.* Glycine betaine and proline betaine in human blood and urine. *Biochim Biophys Acta* 1994; 1200: 259–264
39. Pummer S, Dantzler WH, Lien Y-HH *et al.* Reabsorption of betaine in Henle's loops of rat kidney in vivo. *Am J Physiol Renal Physiol* 2000; 278: F434–F439
40. Kempson S. A, Montrose MH. Osmotic regulation of renal betaine transport: transcription and beyond. *Pflugers Arch* 2004; 449: 227–234
41. Grunewald RW, Oppermann M, Schettler V *et al.* Polarized function of thick ascending limbs of Henle cells in osmoregulation. *Kidney Int* 2001; 60: 2290–2298
42. Jouret F, Leenders J, Poma L *et al.* Nuclear magnetic resonance metabolomic profiling of mouse kidney, urine and serum following renal ischemia/reperfusion injury. *PLoS One* 2016; 11: e0163021
43. Wei Q, Xiao X, Fogle P *et al.* Changes in metabolic profiles during acute kidney injury and recovery following ischemia/reperfusion. *PLoS One* 2014; 9: e106647
44. Al-Ani B, Fitzpatrick M, Al-Nuaimi H *et al.* Changes in urinary metabolomic profile during relapsing renal vasculitis. *Sci Rep* 2016; 6: 38074
45. Fowler MJ. Microvascular and macrovascular complications of diabetes. *Clin Diabetes* 2008; 26: 77–82
46. Nakagawa S, Nishihara K, Miyata H *et al.* Molecular markers of tubulointerstitial fibrosis and tubular cell damage in patients with chronic kidney disease. *PLoS One* 2015; 10: e0136994
47. Martín-Cleary C, Ortiz A. CKD hotspots around the world: where, why and what the lessons are. A CKJ review series. *Clin Kidney J* 2014; 7: 519–515
48. Clark WF, Sontrop JM, Huang S-H *et al.* Hydration and chronic kidney disease progression: a critical review of the evidence. *Am J Nephrol* 2016; 43: 281–292
49. Eng J, Wilson RF, Subramaniam RM *et al.* Comparative effect of contrast media type on the incidence of contrast-induced nephropathy a systematic review and meta-analysis. *Ann Intern Med* 2016; 164: 417–424

Received: 27.10.2017; Editorial decision: 22.12.2017